LRP 408/90 July 1990

ION CYCLOTRON WAVE EXCITATION BY DOUBLE RESONANCE COUPLING

A. Fasoli, T.N. Good, P.J. Paris,
F. Skiff, M.Q. Tran

ION CYCLOTRON WAVE EXCITATION BY DOUBLE RESONANCE COUPLING

A. Fasoli, T.N. Good, P.J. Paris, F. Skiff+, M. Q. Tran

Centre de Recherches en Physique des Plasmas
Association Euratom - Confédération Suisse
Ecole Polytechnique Fédérale de Lausanne
21, Av. des Bains - CH-1007 Lausanne - Switzerland

+ Permanent address: Laboratory. for Plasma Research, University of Maryland, College Park, MD 20742 USA

Abstract

A modulated high frequency wave is used to remotely excite low frequency oscillations in a linear, strongly magnetized plasma column. An electromagnetic wave is launched as an extraordinary mode across the plasma by an external waveguide in the Upper Hybrid frequency regime $f \approx f_{UH} \approx f_{ce} \approx 8$ GHz, with $P \leq 2$ W. By frequency modulating (at $f_{FM} \approx 1-60$ kHz, with $f_{ci} \cong 30$ kHz) the pump wave, the resonant layer is swept radially across the profile and perpendicularly to the field lines at $f=f_{FM}$. The resulting radial oscillation of the electron linear and non linear pressure can be considered to act as a source term for the ion wave. A localized *virtual* antenna is thereby created inside the plasma. Measurements of the ion dielectric response (interferograms and perturbed distribution functions) via laser induced fluorescence identify the two branches (forward, or ion-acoustic-like, and backward, or Bernstein, modes) of the electrostatic dispersion relation in the ion cyclotron frequency range. By changing the modulation bandwidth, and thus the spatial excursion of the oscillating resonant layer, a control on the perpendicular wavelength of the excited mode can be exerted. In particular, the possibility of selective excitation of the ion Bernstein wave is demonstrated experimentally.

Introduction

The term Double Resonance is normally used to indicate a non-linear wave process involving a high frequency plasma (pump) wave, which corresponds to one of the electron plasma eigenmodes, modulated in frequency or amplitude at a frequency close to a resonance for the ion population (typically, the ion cyclotron frequency in a magnetized plasma)[1]. The Double Resonance has constituted from the beginning one of the possible schemes to launch low frequency waves in a steady-state plasma[1]. In the experiment reported herein, we analyze primarily the mechanism of remote excitation of electrostatic ion waves by an electromagnetic Electron Cyclotron-Upper Hybrid (EC-UH) pump wave.

Research in this domain started as a direct consequence of studies on parametric decay processes. Parametric decay generally refers to the non-linear instability of low frequency and sideband "daughter" waves in the presence of an intense high frequency pump wave[2]. In early experiments, this phenomenon appeared through an anomalous (i.e. exceeding the amount predicted by linear theory) absorption of the pump wave, for instance in the lower or upper hybrid frequency regime[3]. In the latter case, the one of interest for our experiment, a linear conversion of the electromagnetic wave into an electrostatic electron Bernstein wave was also observed[4-6]. The consequent heating effects on electrons had to be taken into account in the energy balance calculations[7]. Later, a low frequency oscillation was detected, which accounted for the extra energy lost by the pump wave. Among the first experimental results was the observation of an upper hybrid wave decaying into an electrostatic electron Bernstein wave and an ion acoustic wave (or waves, since the low frequency spectrum was quite broad)[8-9]. Significant ion heating was found to be directly generated by these oscillations, in toroidal[10] and in Q-machine[11] plasmas. A series of intensive studies, focused on the use of parametric decay as an auxiliary heating scheme, originated from this observation.

On the other hand, those who were dealing with laser-produced plasmas, were trying to understand and avoid an apparent non-linear degradation of the laser pulse energy, which appeared to be dispersed by the effect of parametric instability over a number of decay plasma modes. Both programs were led to the same question: what happens if a non-monochromatic (e.g. amplitude or phase modulated) wave is injected into the plasma instead of the usual single frequency pump wave?

Those who were studying the parametric decay as a possible auxiliary heating scheme for magnetized plasmas, tried to modulate the pump wave in order to lower the threshold power for the occurrence of the decay, and to increase the saturated level of the ion instability. Oppositely, in the domain of laser-produced plasmas, a method of increasing the threshold and eventually reducing the saturated level was sought. Curiously, a way to achieve the desired result (a reduction or an increase of the threshold, respectively) was found in both cases.

In particular, an enhancement in the ion oscillation and the related ion heating was noticed in experiments where, by amplitude modulation, the difference in the frequency of the two pump waves was of the order of (or twice) the so-called ion acoustic frequency[12] ($\Omega_0 = kc_S\ (1 + k^2/k_D^2)^{-1/2}$, where k is the wavenumber, $k_D^2=(4\pi ne^2)/T_e$, and c_S is the ion-acoustic speed). This represented a confirmation of the non-linear Vlasov theory which predicted a lowering of the threshold when the linear electron wave damping rate is either much larger[13] or much smaller (in a magnetized plasma)[14] than the ion acoustic frequency. In the case of frequency modulation, a bandwidth of the pump wave much larger than the resonance width for the instability was found to increase the threshold and decrease the growth rate[15]. No clear conclusion for the effect of a bandwidth comparable to or smaller than the resonant frequency interval on the growth rate has been found in the literature.

More recent theories determine the limits of validity of the original analysis of Arnush et al.[13] (e.g. a temperature ratio T_e/T_i larger than 5 is required)[16], and try to solve the apparent contradictions in the previous results[17]. Both the cases of amplitude and frequency (or phase) modulation were treated. The change in the threshold field amplitude for the two types of modulation with respect to the monochromatic case is calculated for the parametric decay into longitudinal waves. A reduction of the decay effects is found for the FM case, essentially due, as in reference 15, to the spread of the wave energy over an entire range of frequencies. On the other hand, the threshold for the AM case is predicted to depend directly on the ratio between the period and the pulse width of the modulation signal.

Of more general interest, since it does not depend on any particular assumption needed for a non-linear theoretical model, is the result of an experiment dealing with a pump frequency above the lower hybrid resonance[18]. The amplitude modulation can have a stabilizing or destabilizing effect with respect to the monochromatic decay instability, depending on whether the variation of the wave amplitude is rapid or slow (compared to the

time scale of the ion cyclotron period), respectively. Moreover, a strong response, mostly in terms of ion heating, has been found in linear magnetized plasmas for a modulation frequency approaching the ion cyclotron frequency or its first harmonics[18-19].

Beyond the heating applications, in tokamak plasmas[20] (limited by a poor overall energetic efficiency), renewed interest in the Double Resonance as a wave launching scheme has recently been shown, in connection with experiments on large scale modifications of the ionosphere by electromagnetic waves[21], including a proposal to limit the ozone layer destruction rate by the action of ground-launched electromagnetic waves[22]. In laboratory plasmas, an additional method for the excitation of ion modes may reveal new features of the wave-particle interaction phenomena.

In this context of remote excitation of low frequency waves, we study the modulated high frequency resonance as a kind of virtual antenna for the electrostatic ion cyclotron waves, both the forward (or ion acoustic-like) and the backward (or neutralized Bernstein) modes. A method for the selective excitation of the latter, based on an appropriate choice of the modulation parameters, is proposed.

The paper is organized as follows. In the first section we shall describe the experimental apparatus, the RF circuit and the laser diagnostic used to detect the ion oscillation. Part 2 will treat the case of the monochromatic wave, the related "classical" parametric processes and the consequent heating effects; the high frequency wave effects which could act as source terms for the ion wave will be pointed out. In the third chapter the results on the ion wave excitation via a modulated pump will be presented and a simple theoretical model will be suggested. The general features of the experimental results and possible applications of this wave scenario will then be discussed and proposed in the conclusive section.

1. Experimental set-up and diagnostic apparatus.

The experiment is performed on the Linear Magnetized Plasma (LMP) Q-device[23]. The plasma is produced by contact ionization of a barium vapor jet on a rhenium-plated tungsten hot plate[24]. The resulting plasma column has a length of about 5 m and a diameter of 5 cm. Densities are of the order of 10^9-10^{10} cm^{-3}. Electron and ion temperatures are determined by the independent equilibria of the two plasma species (barium singly ionized ions and electrons) with the vaporizing assembly: $T_e \cong T_{i\perp} \cong 2T_{i\parallel} \cong 0.2$ eV. A sheath acceleration at the hot plate causes a supersonic drift for ions of about $v_D \cong 1.2 \times 10^5$ cm/s. The axial magnetic field ($B \approx 0.3$ T, corresponding to $f_{ce} \approx 8$ GHz, $f_{ci} \approx 30$ kHz) is characterized by spatial

and temporal variations smaller than 0.1%. Inhomogeneities in time or space (except the radial temperature and density profiles) for the plasma parameters are kept below 1%.

The RF launching apparatus is composed of a high frequency (7-12 GHz) generator, with inputs for Amplitude and Frequency Modulation (AM, FM), a Traveling Wave Tube Amplifier (TWTA), and an open X-band waveguide facing the plasma at a distance of about 1 cm, inside the vacuum chamber. The so-called X-mode is used, in which the wave electric field is perpendicular to the static B-field. A second open waveguide is placed in front of the antenna to measure the transmitted power through the plasma slab. The output power after the TWTA can be varied from 0 to 40 dBm. The coupling to the plasma is roughly estimated by measuring incident and reflected power at the feedthrough connecting the line to the waveguide-antenna. The maximum power flux to the plasma is of the order of 1 W/cm^2. The natural jitter in frequency of the microwave source is below 3 MHz. In FM, the source field can be represented in the form $E_0\cos[t(\omega_0+\Delta\omega\cos\omega_{FM}t)]$, where ω_0 is the central (or "pump") frequency, ω_{FM} the modulation frequency, and $\Delta\omega$ the modulation "excursion". A modulation $\omega_{FM}<50$ kHz , with an excursion $\Delta\omega$ between 0 and 30 MHz, can be obtained. The frequency bandwidth for the AM case is much larger, and covers several ion cyclotron harmonic bands. A schematic view of the RF circuit is shown in fig.1, along with the lay-out of the LMP device and the geometry of the launching system.

The diagnostic apparatus is mainly devoted to the study of the low frequency (i.e. ion) features. Besides a number of standard single tip electrostatic probes, it is based on the technique of Laser Induced Fluorescence (LIF)[25]. A cw narrowband laser beam, traversing the plasma perpendicular or parallel to the magnetic field, induces a quantum transition of the barium ions. By looking at the light emitted by de-excitation, a direct measurement of the ion distribution function (via Doppler shift for the different ion velocity classes) and the related moments (density, temperature, drift velocity, etc.) is possible[26]. Magnetic fields can be estimated from the Zeeman splitting of the emission line. The spatial resolution for the LIF measurement is determined by the intersection between the laser beam and the viewing volume of the detection optics (typically, few mm^3). The time response depends primarily on the excited state lifetime; for the line chosen in the case of the singly ionized barium ($6^2P_{1/2}$ decaying to the ground state, $6^2S_{1/2}$) it is of the order of 10 nsec. The electronics used for the data acquisition (a standard Photo Multiplier Tube and a fast response amplifier system) reduces this temporal resolution by a factor of 10. A scannable optical carriage allows injection of the laser beam and

detection of the induced fluorescence at different axial positions, over a plasma length of more than 150 cm[27].

In the case of collisional pumping of the quantum states, a measurement of the density of the excited states enables one (via an assumption on the form of the electron distribution) to infer the electron temperature[28]. The time response remains the same as for the LIF active measurements, but spatially the recorded light signal is emitted all along a radial chord of the plasma cross section. Nevertheless, on the z-axis, a resolution of about 3 mm is achievable, corresponding to the section of the observed plasma volume.

2. The monochromatic high frequency wave.

In this section we focus our attention on the propagation and the parametric decay of the monochromatic high frequency wave. As mentioned before, we operate in the frequency range of the upper hybrid resonance ($f_{UH}^2 \approx (f_{ce}^2+f_{pe}^2)^{1/2} \approx 8$ GHz). For a low density, relatively strongly magnetized plasma, $f_{pe} << f_{ce}$, and f_{UH} is very close to the electron cyclotron frequency: $\Delta f = f_{UH} - f_{ce} \approx 1/2\ f_{pe}^2/f_{ce}$ ≈ 50 MHz ($\Delta f/f \approx 0.6$ %).

It is well established, both in theory and in the experiments, that when an electromagnetic wave propagating in the X-mode encounters the upper hybrid resonance, the electric field is enhanced in amplitude and tends to become parallel to the direction of propagation[4-7]. The condition for matching to the electrostatic mode is then satisfied, and an efficient conversion to the Electron Bernstein (EB) wave can take place. To confirm this picture for our particular plasma parameters, we consider the warm (i.e. first order in Larmor radius) plasma dispersion relation for an e.m. wave in the upper-hybrid frequency range. A typical solution is shown in fig.2 as a function of the radial position on the density profile. The analytical form $n(r)=n_0[1+ \exp(\alpha r-\beta)]^{-1}$, with $\alpha=5.6$ cm^{-1} and $\beta=10$ to fit the experimental profile, was considered for this calculation. The upper hybrid layer is clearly identified (the index of refraction tends to infinity); at that point of the profile, the wave characteristics become electrostatic (large refraction index), and almost independent of the density.

Propagation for the EBW is allowed between the electron cyclotron and the upper hybrid frequency, only. In this range, experimental evidence for the presence of an electrostatic oscillation at the plasma center was found. An L-tip tungsten probe measured effective perpendicular wavelength of the order of 1 cm ($k_\perp \rho_e \cong 2.2\times10^{-3}$), corresponding to typical values for the electron

Bernstein mode. The enhancement of the wave electric field at resonance, limited mostly by the presence of collisions, as predicted theoretically[29], is responsible for a strong local electron heating. The situation is somewhat complicated by the presence, between f_{ce} and f_{UH}, of the conversion-originated EBW. The propagating electron Bernstein wave, in fact, can give energy to the electrons via linear (cyclotron or Landau) damping mechanisms. Moreover, for $f=f_{ce}$, the Electron Cyclotron Resonant Heating (ECRH) can occur all along the plasma cross section. We will see in the next section, though, that the plasma response seems well localized, indicating that this effect does not play a predominant role. For these reasons, in addition to the natural narrowness of the frequency range for propagation, the whole interval $[f_{ce}, f_{UH}]$ will be considered in the following to be *the* resonant region. Different tools are used to locate the resonance, based mostly on the heating effects manifested by the wave in that frequency domain.

First, the presence of relatively high energy electrons can be detected in the Barium plasma by looking at the light emitted by the ions at 493.4 and 455.4 nm. These wavelengths correspond, in fact, to the transitions to the ground state from the first excited states $6^2P_{1/2}$ and $6^2P_{3/2}$, respectively. The corresponding energy is about 2.5 eV; a collisional pumping of those states (and, of course, the successive radiative decay) is then possible only where and when the electron distribution function contains a finite number of particles endowed with 2.5 eV, or more, of kinetic energy. Assuming a Boltzmann electron distribution, one can get a value for the temperature (or pseudo-temperature T_e^*, since the dependence on the a priori assumption on the distribution is essential) by comparing the intensity of the two spectral lines. Variations in the electron temperature can be followed by looking at the Langmuir probe characteristics, with an enhanced spatial resolution (<3 mm) but a relatively slow time response. The high frequency resonance can also be found by measuring the transmitted power through the plasma slab: the enhanced absorption of the pump wave will cause a dip in the microwave transmission signal. The three signals (ion saturation current from the probe, proportional to the product $n \times T_e^{1/2}$, plasma fluorescence at 493 nm, and transmitted microwave power) are presented versus the frequency of the e.m. wave in fig.3. The width of the resonant region is about 50 MHz, as expected, and it is almost independent of the incident power.

The scaling of T_e^* with the RF incident power is displayed in fig.4. A significant ($T_e^*{}_{max}/T_0 \approx 40$) electron heating (or, in the case of a non-maxwellian distribution, process of creating suprathermal electrons) is evident. The possibility of controlling the T_e^* value is

demonstrated as well, despite of the fact that no simple explanation for the 1/2 power dependence has been found.

The strong electric field at resonance can give rise to local ponderomotive force, acting directly on electrons, and via the ambipolar field, on ions. A consequence could be the formation of density cavities at the resonance location[30]. This is a possible explanation of the sharply peaked T_e^* axial profile shown in fig.5a. More likely, the bump in T_e^* is a consequence of the relaxation of the heated electron distribution into a maxwellian. The classical conductivity along the field lines, in fact, would not support such a strong energy gradient in proximity of the external waveguide launcher. It has to be underlined that for this measurement the experimental conditions are different with respect to the case of fig.4; in particular, the background neutral density is higher (almost by an order of magnitude), giving rise to a number of possible loss channels for the injected wave energy. For the same nominal input power, effectively, the heating effects appear drastically reduced.

It is here worth mentioning another effect of the high frequency field at resonance, when the background neutral density is comparable to the plasma density. At high RF power, an extra ionization of the residual gas (mostly nitrogen) is observed. The plasma profile is then modified, and the steady-state potential is rearranged. The static electric field increases in amplitude, enhancing then the E×B drift. The LIF ion diagnostic allows us to measure the consequent plasma rotation velocity and associated ion heating due to momentum transfer through collisions[31] (fig.5b). This phenomenon must be taken into account carefully when studying linear and non-linear heating effects of the high frequency wave on the ion population.

Before we address to the case of the modulated electromagnetic wave, we summarize here the observed features of the monochromatic parametric decay. On the low frequency fluctuation spectrum, for instance of the fluorescence (i.e. the ion density), a signal around the ion cyclotron frequency and its harmonics is clearly seen. By measuring the perpendicular wavelength and by testing the frequency dependence of that oscillation on the B-field magnitude (see fig.6a), we identify the decay product as an Electrostatic Ion Cyclotron (EIC) wave ($f^{decay} \approx (1+\delta) f_{ci}$, $\delta \cong 0.2$). The high frequency daughter wave is too close in frequency to the "pump" to be detected directly on the spectrum analyzer ($\Delta f/f \cong 10^{-6}$). Nevertheless, we speculate that the high frequency decay product belongs to the same branch of the dispersion relation as the pump wave; that is the EBW, which in turn is generated by the upper hybrid wave via linear conversion[2]. This kind of decay is observed to be responsible for ion heating (via cyclotron or Landau

damping of the low frequency oscillation). The measured ion temperature and the amplitude ($\delta n/n$) of the decay product are shown in fig.6b as functions of the RF pump power. The convective instability threshold can be situated around 20 dBm.

3. Low frequency wave excitation by modulation of the high frequency resonance.

The central part of our experiment is the study of the excitation of ion oscillations by the modulated high frequency wave at the upper hybrid resonance.The main practical difficulty encountered in the experiment, and the main factor limiting the signal to noise ratio for the majority of the measurements is the stability of the high frequency resonance. We have seen that the width of the resonant frequency interval is less than 0.6% of the driving frequency. Consequently, a stability better than 0.6% is required for both the plasma density and the magnetic field intensity. Since this represents the instrumental limit of our apparatus, particular stratagems (like a feed-back control of the pump frequency from a Hall-probe, for instance) have to be used in the experiment.

A feature already pointed out by Wong et al. in 1970[1] is the resonant plasma response at a modulation frequency coinciding with the ion cyclotron frequency or its harmonics. At lower frequencies, drift and "edge" modes were observed as well. We show in fig.7 the ion response (detected by a floating electrostatic probe) as a function of the modulation frequency, in FM (a) and AM (b), when the high frequency pump is kept at resonance. The measurements via LIF, in fact, are not suitable at the same power level, because of the depletion effect of suprathermal electrons on the metastable state density. It has to be noted that the two measurements, for AM and FM, are intrinsically different: the response shown in FM consists essentially of the magnitude of a signal locked to the FM driver, swept in frequency, while, for the AM case, we show simply the Fourier power spectrum of the probe signal, for an AM frequency coinciding with the decay frequency. Several observations can be made. Both low frequency ($\approx$10 kHz) components and a response around f_{ci} are visible. The low frequency modes are more pronounced in the FM spectrum; in this case the resonance affects, on the average, a broader radial portion of the plasma column. Drift and edge modes may then be more easily driven than in the AM case, since they correspond to macroscopic motion of a finite fraction of the plasma volume.

In FM, the width of the response around f_{ci} (FWHM $\approx$35% of the harmonic band, to be compared to the $\approx$15% characteristic of the

analogous measurement in AM) seems to indicate a relatively broad propagation region for the ion disturbance induced by the pump wave. This propagating feature in FM is confirmed by the displacement of the response on the frequency axis; the minimum damping for the EIC wave corresponds to a frequency range well inside the harmonic band. In the AM case a response at $2f_{ci}$ is seen as well, while no clear signal was detected in AM around $3f_{ci}$ (not shown). In FM, we limited our analysis to the first ion cyclotron harmonic band, since the RF generator does not allow any frequency modulation above 50 kHz ($1.8f_{ci}$).

To demonstrate definitely that the signal observed around the ion cyclotron frequency (the one we are interested in) is effectively due to the high frequency resonance, we fix the modulation frequency ($f_{FM}=\omega_{FM}/2\pi$) and look at the ion response while sweeping the central frequency ($\omega_0/2\pi$). We find again only a narrow region where the signal is above the noise level, confirming the two-coupled-resonance character of the interaction (fig.7c). The double peak structure of this curve may be attributed to the presence of the two distinct resonances (f_{ce}, f_{UH}), at one point on the radial density profile.

In fig.7b, corresponding to the case of amplitude modulation, the spectrum of the ion response without modulation is plotted on the same frequency axis. Along with the low frequency "natural" oscillations around 10 kHz, a peak at $f \approx f_{ci}$ is present even in this case. From a direct comparison on the graph, we can affirm that the amplitude modulation changes only by a small amount the level of the decay instability. A more pronounced effect is induced by frequency modulation: an enhancement of 10 to 15 dB on the signal around f_{ci} is measured with respect to the monochromatic case, for a range of pump powers.

The scaling of the response in FM with the RF power is shown in fig.8. The set of data we refer to corresponds to a time-of-flight measurement (pulsed modulation signal, probe displaced a few cm from the resonant layer); the signal to noise ratio for the ion oscillations is remarkably improved. The dependence seems to be linear, as indicated by the line drawn on the graph; only above 1 W there is a tendance for the points to lie all below the line, indicating a possible saturation effect at high power.

Generally, in our experimental environment, the modulation of the pump wave tends to decrease the instability threshold and enhance the level of the ion oscillation above threshold. In particular, the FM scheme seems relatively efficient for the excitation of the low frequency plasma oscillations. This appears to be in contrast to previous theories treating the change in the threshold for non-monochromatic waves. Our case, actually, is

slightly different from the one analyzed in the theory since the modulation bandwidth never exceeds the resonance width.

More generally, we believe that the excitation of the ion wave by a modulated resonance is not simply a particular case of the parametric decay instability, but represents in itself an independent physical mechanism. To understand it, we study in detail the case of frequency modulation; this scheme is not only favorable from the point of view of the coupling efficiency, but it is also characterized by particular features concerning the excited ion wave.

The frequency modulation of the pump wave is translated, via the condition $\omega=(\omega^2_{ce} + \omega^2_{pe}(r))^{1/2}$, into a radial sweep of the resonant layer. The total radial displacement is simply determined by the modulation excursion. The ratio between the two quantities is a function of the position: $\Delta r \cong (\partial\omega_{UH}(r)/\partial r)^{-1} \Delta\omega$. The strongest coupling occurred generally at the maximum of the density gradient; at that location, a $\Delta\omega$ between 0 and 20 MHz gives a Δr ranging from 0 to a full plasma diameter. In fig.9 we demonstrate a direct dependence of the resonance width on the modulation excursion: the FWHM of the time averaged radial profile of the ion response varies according to the value of $\Delta\omega$. Two resonant layers are visible, indicating a coupling on both slopes of the profile (the waveguide launcher is on the left side, accounting for the peak asymmetry). It is then possible to control, by simply acting on ω_0 and $\Delta\omega$, the location and the radial extension of the resonant region inside the plasma.

To determine the dependence of the amplitude of the ion disturbance on the modulation excursion, a measurement was made of the induced δn at $f_{FM}\cong 20$, kHz while varying $\Delta\omega$. The modulation frequency in the laboratory frame was chosen below f_{ci} in order to deal with one mode only (the ion-acoustic), deferring the question of the energy sharing between the two EIC branches to a later analysis. The result is shown in fig.10. The data points lie fairly regularly on the interpolated line. A simple qualitative model can be discussed to explain the data: consider a potential barrier for the ions, generated by the high frequency resonance and oscillating radially. Selecting the modulation frequency fixes the period required for a complete excursion, back and forth, of the potential barrier. The barrier velocity v_{barr} will then be determined by the total distance which has to be covered, linked, in its turn, to the FM excursion. Finally, v_{barr} is directly proportional to $\Delta\omega$. Now, the linear dependence evident in fig.10 could be explained if the coupling of the ion oscillation is proportional to the intensity of the "kick" given by the potential structure to the perpendicular ion

distribution function, that is to the velocity of the barrier, and consequently to the modulation excursion.

So far, we have been talking about "ion oscillations" or "disturbances", without specifying the wave character of these modes. To investigate this, a technique based on the LIF measurements, the ion dielectric response[32], is applied. This consists essentially in detecting selectively the component of the ion fluorescence (for each velocity class, separately, and for the integrated distribution) which oscillates in phase or in quadrature with the driving source (in our case, the modulation signal). In LIF, when the laser beam is directed to the plasma on the parallel (perpendicular) direction, a measurement of the ion distribution integrated over perpendicular (parallel) velocities is "automatically" performed. This represents a sensitive, non-perturbative method to record perpendicular and parallel interferograms. By applying this technique to the frequency modulated upper hybrid wave, the launched ion wave dispersion relation is reconstructed experimentally.

We show in fig.11 the measured perpendicular dispersion relation, corresponding to the given parameters; the modulation excursion has been kept constant all along the series of measurements. Points corresponding to several experimental runs (characterized by slightly different values of the magnetic field and density) are displayed. The scattering of the points is increased by the "instrumental" instability of the high frequency resonance mentioned in section 2. The horizontal error bars are linked to the measurement of the parallel wavelength ($0.1\ cm^{-1} < k_{\|} < 1.5\ cm^{-1}$); since the plasma drifts along the magnetic field lines at a velocity v_D, the frequency in the plasma frame is effectively Doppler shifted: $\omega \Rightarrow \omega \pm k_{\|} v_D$.

The theoretical electrostatic dispersion relation in the regime of interest here ($v_{thi} < \omega/k_{\|} < v_{the}$) exhibits two separated roots: the forward branch (called also ion-acoustic-like, since it is affected very weakly by the B-field) and the backward (or Neutralized Ion Bernstein, NIB) mode. A set of solutions calculated from the linear electrostatic dispersion relation for a possible range of plasma and wave parameters is shown as a theoretical "band" on the same graph. Both modes can be identified, and their crossing point (where the real parts of the wavenumber coincide), can be situated in a region where $k_{\perp}$ is of the order of $10\ cm^{-1}$.

A general problem encountered in low frequency wave studies in basic plasma physics is the difficulty in exciting the Bernstein wave; for capacitive antennas[33,34], for instance, the excitation efficiency for the slow wave is usually much smaller than for the fast (forward) wave. In the Double Resonance scheme, on the

contrary, the $\delta n/n$ corresponding to the two modes is of the same order of magnitude (never exceeding 3 %), for the maximum modulation excursion. Indeed, the latter quantity plays an important role, as we will see, in determining the relative amplitude of the two modes and eventually the selective excitation of the NIB wave.

The usual strong damping for ion waves in Q-machine, due to a temperature ratio close to unity, is in this case reduced; the heating rate is in fact smaller for ions than for the electron population. The ratio T_e/T_i increases by almost an order of magnitude, and the Landau damping effects decrease significantly. This explains the propagation observed over a portion of the harmonic band much broader than in the unheated case[35].

The clearest signature of an ion wave propagating in a plasma is the first order perturbed ion distribution function ($f^1(v_{\parallel},v_{\perp})$). A series of measurements of $f^1(v_{\perp})$ was recorded, for different experimental conditions. From the form of the perturbed distribution function, several pieces of information about the character of the oscillation can be extracted. In particular, by comparing the data with the result of a Vlasov model, the character of the wave, and indirectly of the mechanism generating it, can be extrapolated. A typical measurement of $f^1(v_{\perp})$ in the FM case is shown in fig.12, for $f_{FM}=1.3f_{ci}$. The velocity space oscillations are characterized by a certain equivalent wavelength and corresponding wavenumber, $K_{v\perp}$. Thinking in terms of the theoretical solution for f^1 in the case of a linearly excited electrostatic plane wave, a direct correspondence between $K_{v\perp}$ and the actual wavenumber $k_{\perp}$ (Fourier conjugated to the real coordinate r) can be established[32]: $k_{\perp}\approx 2\pi f_{ci}K_{v\perp}/v_{thi}$. A good agreement between the value of the wavenumber derived from the velocity space oscillations of the perturbed ion distribution and the one measured macroscopically by interferometry has been found for several driving (i.e. modulation) frequencies. The similarity with the linear e.s. case suggests that the explanation of the Double Resonance (DR) ion wave excitation scheme should be sought in the frame of the Vlasov-Poisson description.

No clear signal corresponding to $f^1(v_{\parallel})$ was observed. In fact, what characterizes the action of antennas inserted in the plasma column is the creation of a ballistic perturbation on the distribution, which propagates parallel to the magnetic field. This is particularly evident in the case of a grid covering the plasma cross-section; "bursts" of particles are created at the driving frequency, and free-stream away from the grid location. The parallel ion distribution function (both the first order perturbed and the zero order one, if the applied voltage is large enough) is then composed by a set of

pseudo-beams which in some sense mask the collective field response[36]. One of the advantages of the DR as an external launching scheme for electrostatic waves, exempt from mechanical structures inside the plasma, is the possibility of avoiding ballistic perturbations.

We demonstrated that the oscillating upper hybrid resonant layer plays the role of a "virtual" antenna localized on the perpendicular density gradient. To have a better comprehension of the physical properties of this launcher, a simple theoretical model can be sketched. The observed ion wave features suggest the use of a Vlasov model. The strong local electron heating produced by the high frequency wave, on the other hand, seems to individuate the most effective source term for the low frequency wave in radial gradient of the electron temperature (∇T_e).

By assuming quasi-neutrality and an adiabatic (or Boltzmann-like) electron response, one can postulate for the driving potential the expression:

$$\Phi(\underline{r},t) \cong \frac{k_B}{e} T_e(\underline{r},t) \int d\underline{v}\, f^1{}_i(\underline{r},t,\underline{v}) \qquad (\underline{r}=(r,\theta,z)),$$

where $f^1{}_i(\underline{r},t,\underline{v})$ is the first order perturbed ion distribution and k_B the Boltzmann constant. The temperature term can be taken of the form:

$$T_e(\underline{r},t) = T_e{}^0[1+\tau\, \delta(z-z_0)\, \delta(r-r_0+\Delta r \cos \omega_{FM} t)],$$

where (r_0, z_0) is the resonance location and $\tau = T_e{}^1/T_e{}^0$ ($T_e{}^1$ is the locally enhanced electron temperature). Starting from the linearized Vlasov equation, Fourier analyzed in time and space and integrated over velocity space, a general form of the equation for the density perturbation (in Fourier space) can be obtained:

$$n^1(\omega,\underline{k})\, D(\omega,\underline{k}) = \tau\, \Delta\, \Sigma_{m,n}\, f_m(\omega, \underline{k}) \int d\underline{k}'\, g_n(\underline{k}', \Delta)\, n^1(\omega + \alpha_{nm}\, \omega_{FM}, \underline{k}')$$

$D(\omega,\underline{k})$ is the standard electrostatic dispersion function; α_{nm} indicates a linear combination of the indices n,m. The functions f_m and g_n contain essentially Bessel functions of argument $k_\perp \Delta$ (or $k_\perp' \Delta$). The source term on the RHS acts like a small perturbation of the linear dispersion relation $D(\omega,\underline{k})=0$. For a fixed frequency, the efficiency of the coupling to the plasma modes is therefore determined by the amplitude of the source function calculated at a point in the $\underline{k}$ space which satisfies the plasma dispersion relation. To a first approximation, $k_\parallel$ can be considered as a free variable:

the most important parameter determining the relative amplitude of the various terms is therefore the value of the product $k_\perp \Delta$. Thus, the perpendicular wavenumbers will be influenced by the resonance excursion Δ, fixed univocally by the frequency modulation excursion.

In fig.13 the measured perpendicular wavelengths are shown as a function of the radial resonance excursion, for a fixed driving frequency ($f_{FM}=1.1\ f_{ci}$). The observed linear dependence of $\lambda_\perp$ on Δ seems to indicate that a value of the product $k_\perp \Delta$ for which the wave excitation efficiency is maximum. Consequently, a control over the launched perpendicular wavelengths and a selective excitation of the ion Bernstein mode (characterized by large values of $k_\perp$) can be achieved experimentally.

Conclusions

A mechanism for the excitation of low frequency electrostatic waves by means of a modulated high frequency (upper hybrid) plasma resonance has been studied experimentally. The excited waves ($f \approx f_{ci}$) have been identified as belonging to the two branches (forward and backward) of the electrostatic ion cyclotron wave dispersion relation.

The analogies and differences with respect to the parametric decay of a monochromatic pump wave have been investigated. The heating effects observed on the ion distribution have been attributed to the classical parametric decay. An increase in the level of the ion oscillation manifested when a modulation (at the decay product "natural" frequency) was applied to the driving field. In particular, by frequency modulation, a 10-15 dB enhancement in the instability level above threshold was noticed.

The "virtual" antenna resulting from the radial sweep of the resonant layer (in FM) has a number of interesting properties. With respect to a metallic antenna inserted into the plasma, it has the advantage of avoiding a direct perturbation of the density and the ion velocity distribution: the coupling takes place only via collective field effects.

By imposing a certain frequency modulation range one can fix the radial excursion of the resonance-antenna. A model, based on Vlasov equation for ions, and on the local electron temperature gradient as a source for the low frequency oscillation, indicates a possible selective excitation of the Bernstein wave. The experiment confirmed this prediction, showing a "control" of the perpendicular

wavelength (exploiting the degree of freedom left by the relative dispersion relation) through the choice of the modulation excursion.

Several applications of this wave scenario can be suggested. First, it can be applied to the study of chaotic wave-particle interaction. The Bernstein mode, in fact, is particularly suitable for experiments on stochasticity, where the transition to a chaotic regime for the ion orbits is tightly linked to the presence of a high $k_\perp$ electrostatic wave[37]. For this application, though, a number of plasma parameters must be modified with respect to the reported experiment, in order to reduce the parasitic effects of the high frequency field (e.g. plasma rotation and heating), and to increase the amplitude (in terms of $\delta n/n$) of the excited low frequency modes. In the case of remote wave excitation in the ionosphere, the performed experiment seems to suggest to explore the possibility of using a frequency (as an alternative to amplitude) modulated ground launched wave.

Considering the diagnostic application of the EIC wave propagation study[34,38], which allows an estimation of the ion temperature from the shape of the dispersion curve, one can finally propose a scenario in which a low power electromagnetic wave is injected from outside in a high temperature (e.g. tokamak) plasma. When a frequency modulation (in the range of the ion cyclotron frequency) is applied, an ion oscillation is excited at the point satisfying the resonance condition. The measurement of the wavenumbers corresponding to different modulation frequencies will then give an estimation of the local value of the ion temperature.

Acknowledgements

The authors would like to express their gratitude to Dr. A. Wong for having inspired this experiment and to Drs X. Llobet, J. Vaclavic and O. Sauter for useful suggestions and discussions.

This work was partly supported by the *Fonds National Suisse de la Recherche Scientifique*, under Grants No. 20-25526.88 and 20-25486.88.

References

(1)- A.Y.Wong, D.R.Baker and N.Booth, *Phys. Rev. Lett.* **24**, 805 (1970).

(2)- M.Porkolab, *Physica* **82C**, 86 (1976).

(3)- A.I.Anisimov, N.I.Vinogradov and B.P.Poloskin, *Sov. Phys. Tech. Phys.* **18**, 459 (1973).

(4)- T.H.Stix, *Phys. Rev. Lett.* **15**, 878 (1965).

(5)- J.Preinhaelter and V.Kopecky, *J.Pl. Physics* **10**, 1 (1973).

(6)- J.J.Schuss and J.C.Hosea, *Phys. Fluids* **18**, 727 (1975).

(7)- B.L.Smith, H.Okuda and H.Abe, *Phys. Fluids* **28**, 1772 (1985).

(8)- B.Grek and M.Porkolab, *Phys. Rev. Lett.* **30**, 836 (1973).

(9)- E.Albers, K.Krause and H.Schluter, *Plasma Phys.* **20**, 361 (1978).

(10)- M.Obayashy, K.Chen and M.Porkolab, *Phys. Rev. Lett.* **31**, 1113 (1973).

(11)- H.W.Hendel and J.T.Flick, *Phys. Rev. Lett.* **31**, 199 (1973).

(12)- A.Akiyama, S.Hirose and S.Takeda, *J. of Phys. Soc. of Japan* **42**, 1715 (1977).

(13)- D.Arnush, K.Nishikawa, B.D.Fried, C.F.Kennel and A.Y.Wong, *Phys. Fluids* **16**, 2270 (1973).

(14)- E.Galin, *Plasma Phys.* **18**, 975 (1976).

(15)- S.P.Obenshain, N.C.Luhmann,Jr., and T.P.Greiling, *Phys. Rev. Lett.* **36**, 1309 (1976).

(16)- B.D.Fried, A.Adler and R.Bingham, *J. Pl. Physics* **24**, 315 (1980).

(17)- V.Stefan, *Phys. Fluids* **26**, 1789 (1983).

(18)- K.Matsumoto and M.Sato, *Plasma Phys. and Controlled Fus.* **26**, 935 (1984).

(19)- M.Okubo, R.McWilliams, R.Platt, D.Sheehan and N.S.Wolf, *Phys. Lett.* **108A**, 252 (1985).

(20)- J.L.Sperling, *Fusion Technology* **7**, 296 (1985).

(21)- A.Y.Wong, P.Y.Cheung, M.J.McCarrick, J.Stanley, R.F.Wuerker, R.Close, B.S.Bauer, E.Fremouw, W.Kruer and B.Langdon, *Phys. Rev. Lett.* **63**, 271 (1989).

(22)- A.Y.Wong, J.Steinhauer, R.Close, T.Fukuchi, G.M.Milikh, *Comments Plasma Phys. Controlled Fusion* **12**, 223 (1989).

(23)- M.Q.Tran, P.Kohler, P.J.Paris and M.L.Sawley, *CRPP Laboratory Report* No. LRP 205/82 (1982) (unpublished).

(24)- P.J.Paris and N.Rynn, *Rev. Sci. Instrum.* **61**, 1096 (1990).

(25)- R.A.Stern, D.N.Hill and N.Rynn, *Phys. Rev. Lett.* **37**, 833 (1981).

(26)- D.N.Hill, S.Fornaca and M.G.Wickham, *Rev. Sci. Instrum.* **54**, 30 (1983).

(27)- F.Anderegg, P.J.Paris, F.Skiff, T.N.Good and M.Q.Tran, *Rev. Sci. Instrum.* **59**, 2306 (1988).
(28)- N.Rynn, E.Hinnov and L.C.Johnson, *Rev. Sci. Instrum.* **38**, 1978 (1967).
(29)- R.B.White and F.F.Chen, *Plasma Phys.* **16**, 565 (1973).
(30)- S.P.Obenschain and N.C.Luhmann, Jr., *Appl. Phys. Lett.* **30**, 452 (1977).
(31)- F.Anderegg, R.Stern, F.Skiff, M.Q.Tran, B.A.Hammel, P.J.Paris and P.Kohler *Phys. Rev. Lett.* **57**, 329 (1986).
(32)- F.Skiff and F.Anderegg, *Phys. Rev. Lett.* **59**, 896 (1987).
(33)- J.Goree, M.Ono, and K.L.Wong, *Phys. Fluids* **28**, 2845 (1985).
(34)- A.Fasoli, M.Fontanesi, A.Galassi, C.Longari and E.Sindoni, *Plasma Phys. and Controlled Fus.* **31**, 313 (1989).
(35)- J.P.M.Schmitt, *Phys. Rev. Lett.* **31**, 982 (1973).
(36)- T.N.Good M. Yamada, A. Fasoli, F. Skiff, P.J. Paris and M.Q. Tran, *to be published.*
(37)- F.Skiff, F.Anderegg, and M.Q.Tran, *Phys. Rev. Lett.* **58**, 1430 (1987).
(38)- G.A.Wurden, M.Ono, and K.L.Wong, *Phys. Rev. A* **26**, 2297 (1982).

Figure captions

Fig.1: (a) lay-out of the LMP-Q machine; the waveguide launcher is visible, as well as some of the diagnostic components.
(b) block diagram of the microwave circuit. A- AM or FM modulation signal; B- main HF generator (7-12 GHz); C- HF spectrum analyzer; D- TWT variable gain amplifier; E- bidirectional coupler; F- open waveguide (X-band); G- vacuum chamber; H- plasma cross section; I- power meter.

Fig.2: Solution of the dispersion relation for electromagnetic waves in a warm magnetized plasma as a function of the position on the density profile ($f/f_{ce}=1.0005$; $f_{UH}(r=0)/f_{ce}=1.025$; $T_e=0.2$ eV; $k_{||}\cong 1\times10^4$ cm^{-1}; $n_e=1\times10^9$ cm^{-3}). The density profile used for the calculation is shown as well (dotted line).

Fig.3: Different signals indicating the high frequency resonance: the transmitted power through a plasma slab (a), the fluorescence emitted by the plasma at 455 nm (b), and the ion saturation current from a Langmuir probe located at the plasma center (c), are plotted vs. the frequency of the pump wave. The central frequency is 8 GHz. $P_{rf}\approx$ 1 W for the three curves. In all cases the vertical axis has arbitrary units.

Fig.4: Dependence of the line intensity ratio (translated here into temperature, T_e^*) on the RF input power. The observation point is a few cm upstream with respect to the waveguide. The best fit line indicates a square root power dependence.

Fig.5: (a) Axial profile of electron temperature from passive spectroscopy. The launcher position is indicated on the graph. The hot-plate is at z=140 cm. $P_{rf}\approx$ 3 W at resonance. A direct comparison with fig.4 on the absolute values of the temperature should be avoided, because of the different experimental conditions (background neutral density, effective coupling of the microwave to the plasma,...).
(b) LIF measurement of plasma rotation. T_i and the energy associated with the rotational motion ($\div v_{rot}^2$) are plotted vs. the radial position. The coincidence of the two profiles is a definite proof that the origin of the ion heating is in this case the rotational motion. T_i at the center is above the background value, 0.2 eV, because of the parametric decay heating effect (the resonance is kept in the central region of the plasma column).

Fig.6: "Monochromatic" parametric decay features.
(a) Scaling of the decay lower frequency with the B-field. The line corresponding to the values of f_{ci} is also plotted.
$P_{rf}\approx$ 1 W at resonance; r/a=0.

(b) Decay amplitude and ion heating effects for several pump power values. The power axis is logarithmic (dBm); the background noise level for the measurement of the mode amplitude is indicated. T_0=0.2 eV.

Fig.7: (a) Floating probe signal "locked" with the FM input vs. f_{FM}. $P_{rf}\approx 1$ W at resonance; r/a=0. The modulation excursion is kept maximum, $\Delta\omega\cong 20$ MHz.
(b) Low frequency power spectrum of the floating probe signal. $P_{rf}\approx 0.3$ W; the curves corresponding to AM (—) and to the unmodulated case (----) are displayed on the same axis. The vertical scale is linear.
(c) Magnitude of the signal locked with f_{FM}=25 kHz vs. the pump frequency detuning from resonance. Only at resonance the "channel" for the low frequency mode excitation by a frequency modulated e.m. wave is open. The parameters are the same as in (b).

Fig.8: Log-log representation of the dependence of $\delta n/n$ for the FM excited mode on the microwave power (f_{FM}=25 kHz).

Fig.9: Time averaged ion response as a function of the radial position. (a): $\Delta\omega\cong 8$MHz. (b): $\Delta\omega\cong 3$ MHz. The other parameters are as in fig.7b. The density profile is shown as well, for visualisation purposes.

Fig.10: δn of the FM excited low frequency mode vs. the radial excursion of the resonance (calculated from $\Delta(r/a)\cong 1/a(\partial\omega_{UH}(r)/\partial r)^{-1}\,\Delta\omega$. The measurement is performed at the resonance location, r/a=0.5, for f_{FM}=20 kHz and $P_{rf}\approx 3$ W.

Fig.11: Perpendicular dispersion relation. The experimental points have been taken for 2.5 kG< B <3 kG, 0< r/a <0.7, $P_{rf}\approx 0.3$ W, and maximum modulation excursion. The set of theory curves corresponds to 0.1 $cm^{-1}< k_{\|} <1.5\ cm^{-1}$, 0.6 eV< T_e <2.5 eV, 0.18 eV<T_i<0.5 eV, $n=10^9\ cm^{-3}$.

Fig.12: First order perturbed perpendicular ion distribution. $K_{v\perp}v_{thi}\approx 2\pi \Rightarrow k_\perp\cong \pi\Omega_{ci}/v_{thi}\cong 17\ cm^{-1}$, which corresponds to the macroscopic measurement (for the same conditions, $k_\perp^{macro}\approx 16\pm 3\ cm^{-1}$). f_{FM}/f_{ci}=1.3, $P_{rf}\approx 0.3$ W, r/a=0.5; $\Delta\omega\cong 8$MHz.

Fig.13: Optical (LIF) measurement of perpendicular wavelengths at f_{FM}/f_{ci}=1.1 vs. the radial excursion of the resonance; the best fit line is drawn through the experimental points. $P_{rf}\approx 0.3$ W; r/a=0.5.

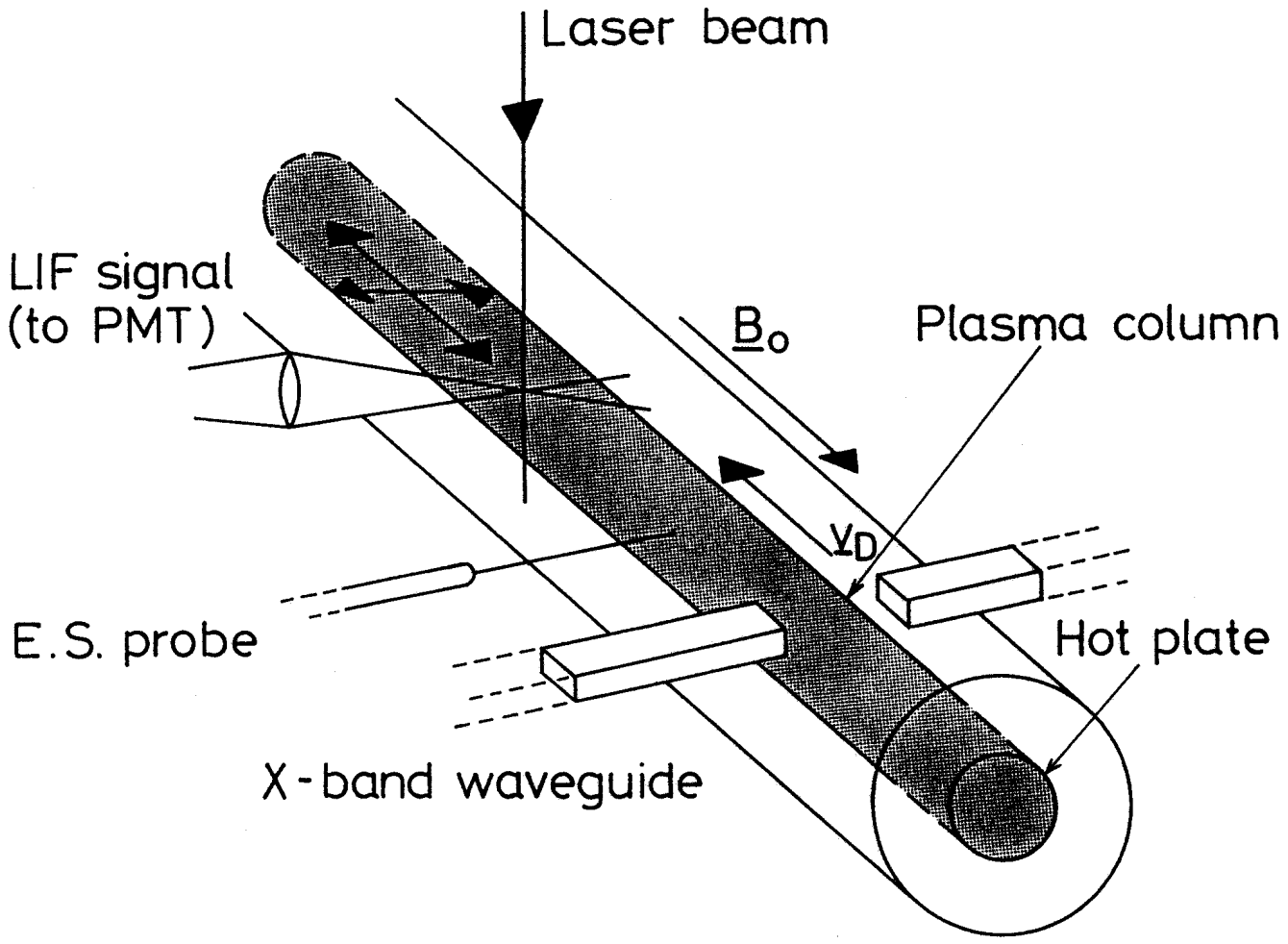
Laser beam
LIF signal
(to PMT)
B_o
Plasma column
v_D
E.S. probe
Hot plate
X-band waveguide

Fig. 1(a)

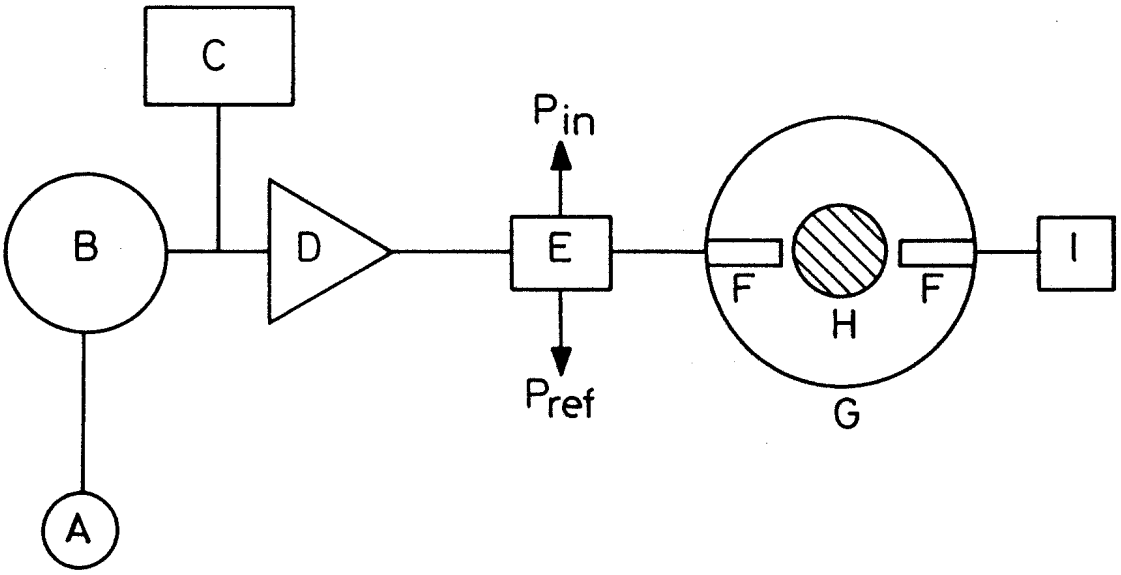

Fig. 1(b)

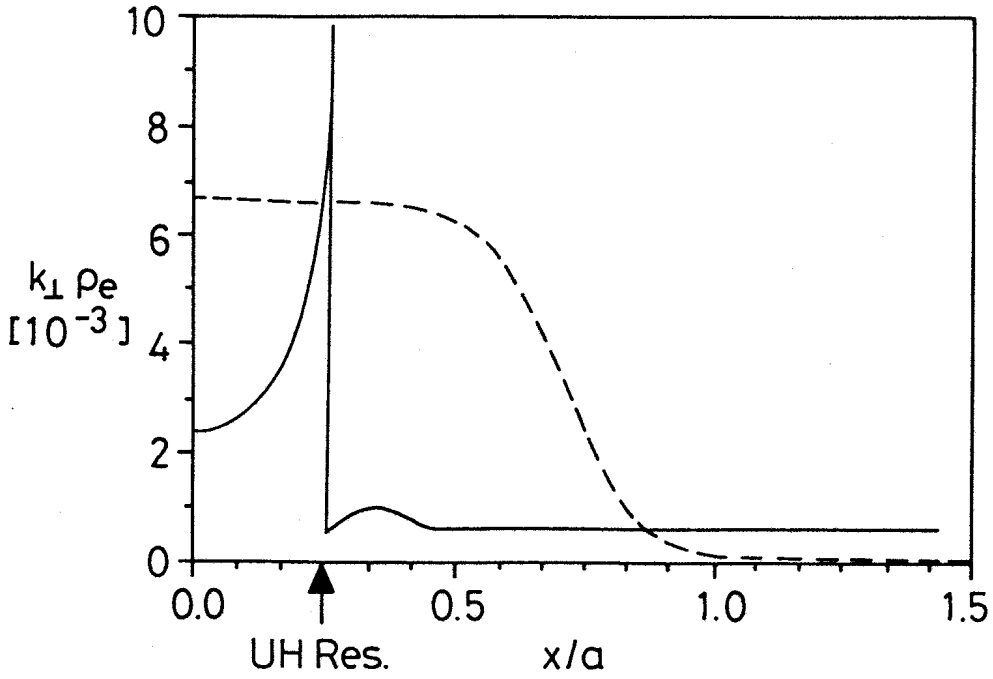

Fig. 2

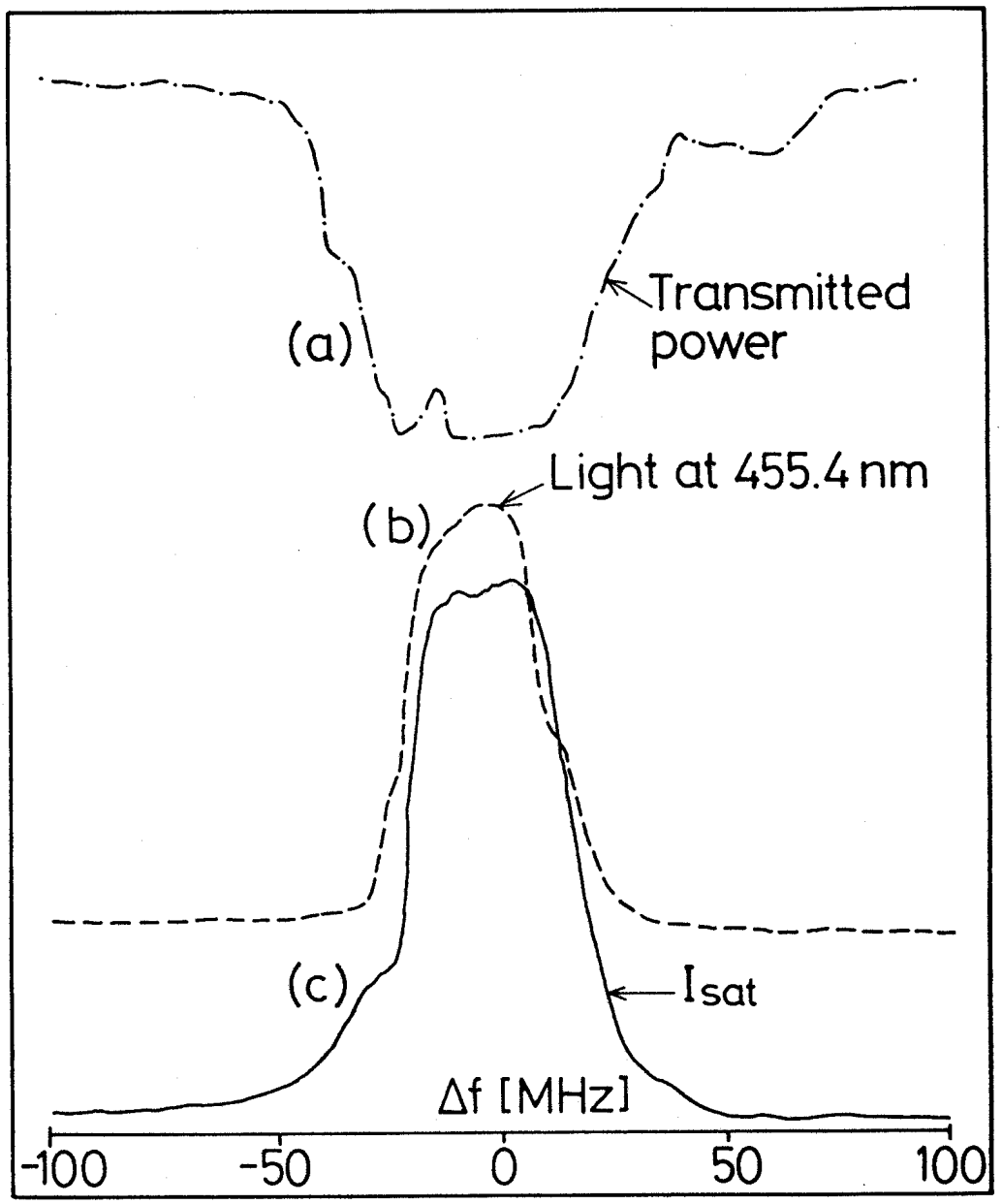
(a)
Transmitted
power
Light at 455.4 nm
(b)
(c)
Isat
Δf [MHz]
-100
-50
0
50
100

Fig. 3

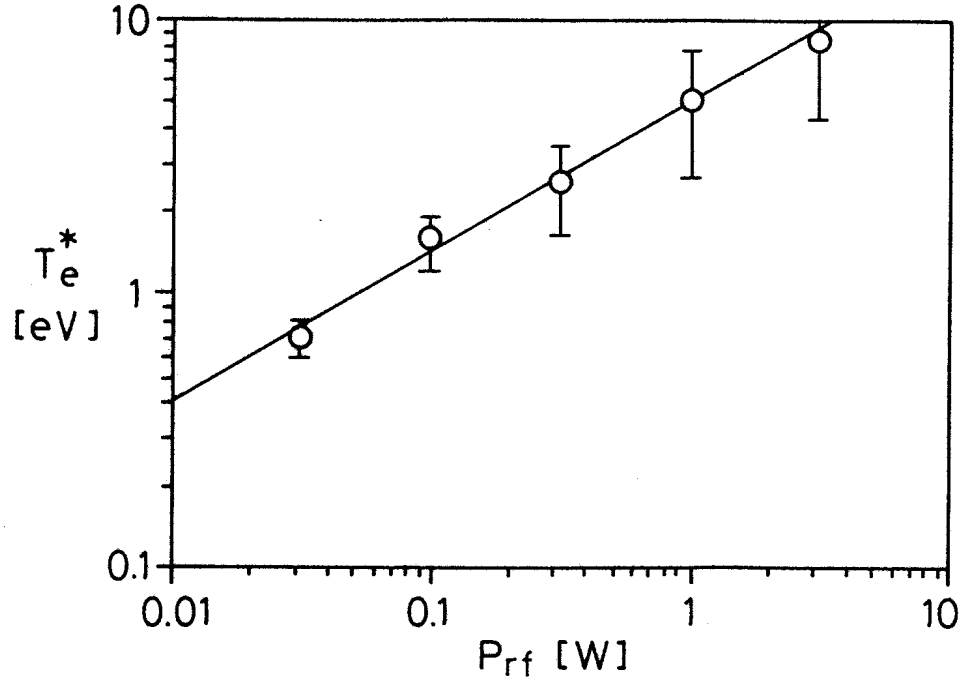

Fig. 4

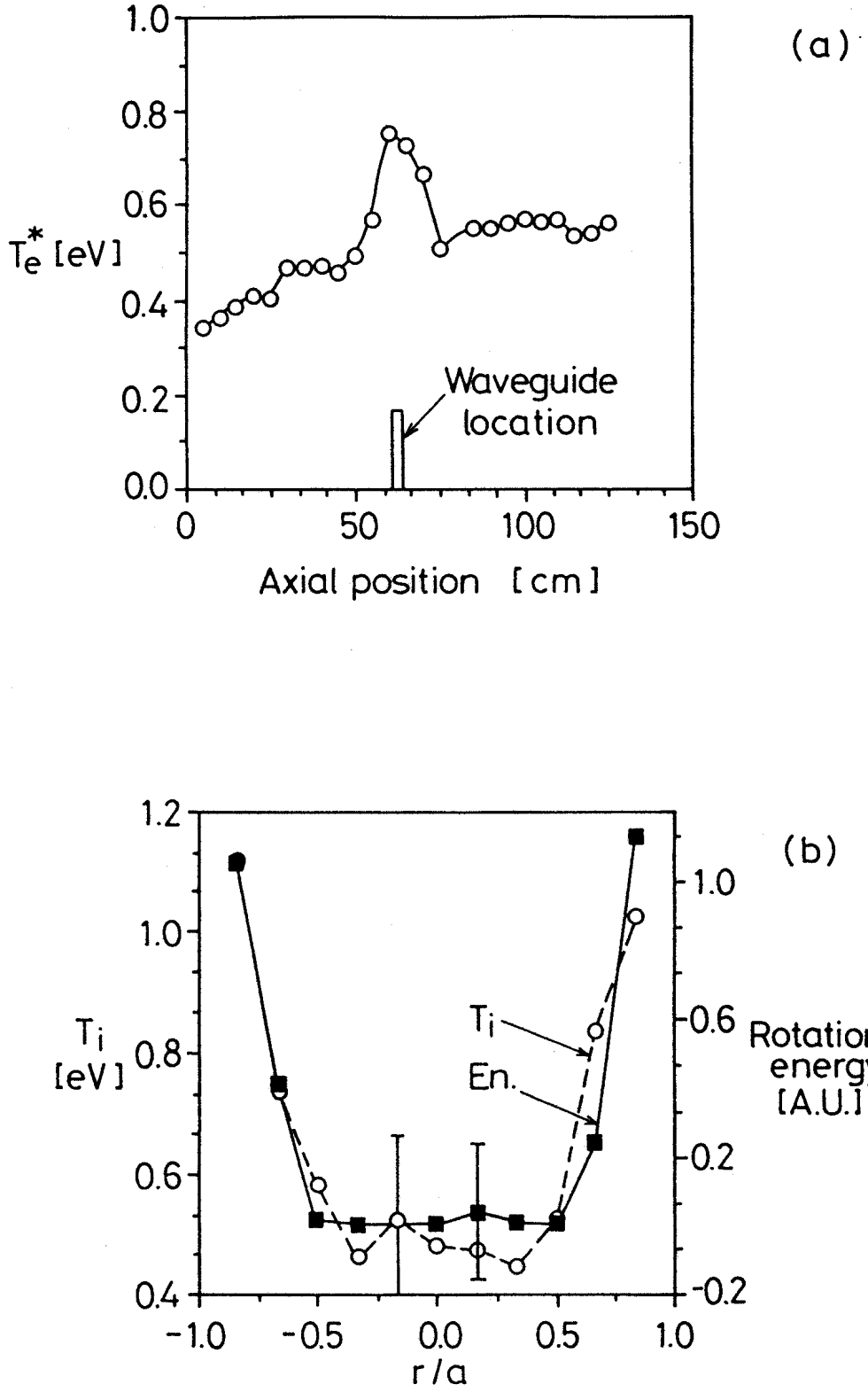
(a)
1.0
0.8
0.6
0.4
0.2
0.0
T_e^* [eV]
Waveguide location
0
50
100
150
Axial position [cm]
(b)
1.2
1.0
0.8
0.6
0.4
Ti [eV]
Ti
En.
1.0
0.6
0.2
-0.2
Rotation energy [A.U.]
-1.0
-0.5
0.0
0.5
1.0
r/a

Fig. 5

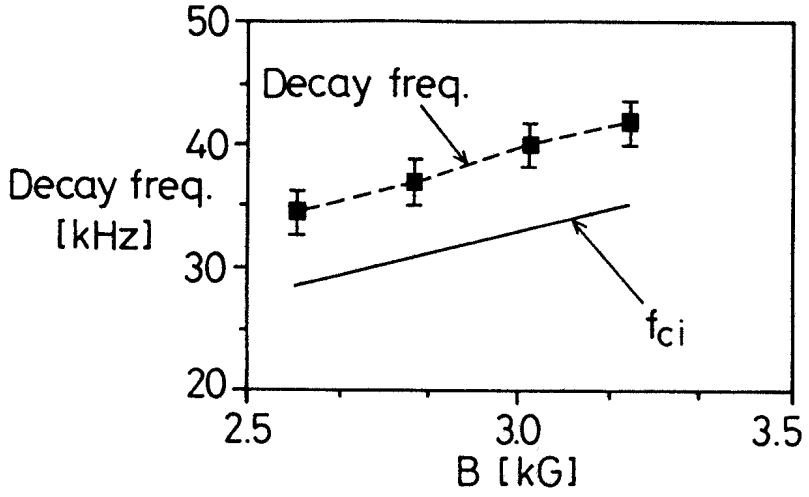
50
40
30
20
Decay freq.
[kHz]
Decay freq.
f_{ci}
2.5
3.0
3.5
B [kG]

(a)

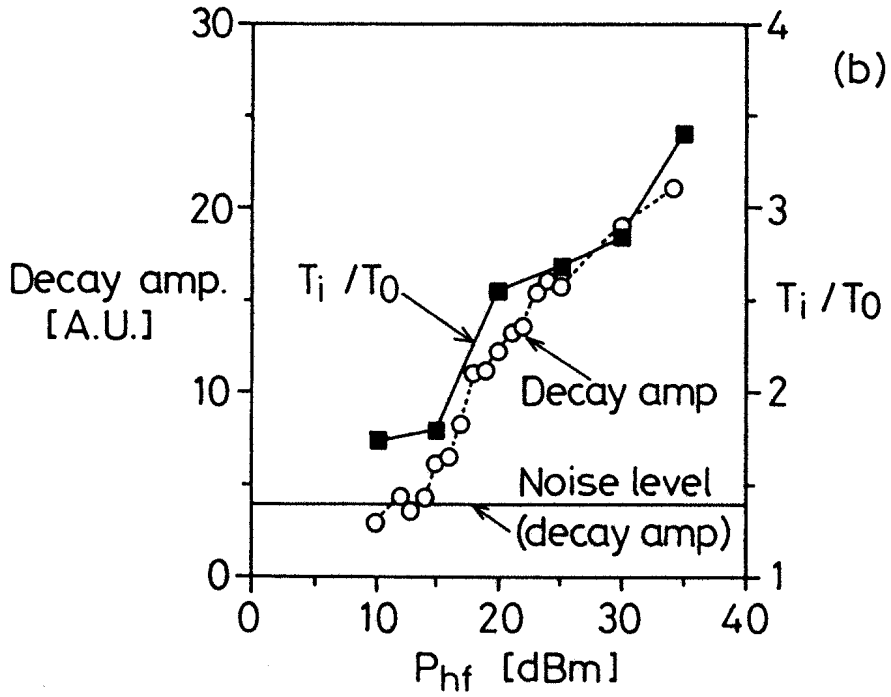
30
20
10
0
Decay amp.
[A.U.]
T_i / T_0
Decay amp
Noise level
(decay amp)
4
3
2
1
T_i / T_0
0
10
20
30
40
P_{hf} [dBm]

(b)

Fig. 6

Fig. 7(a)

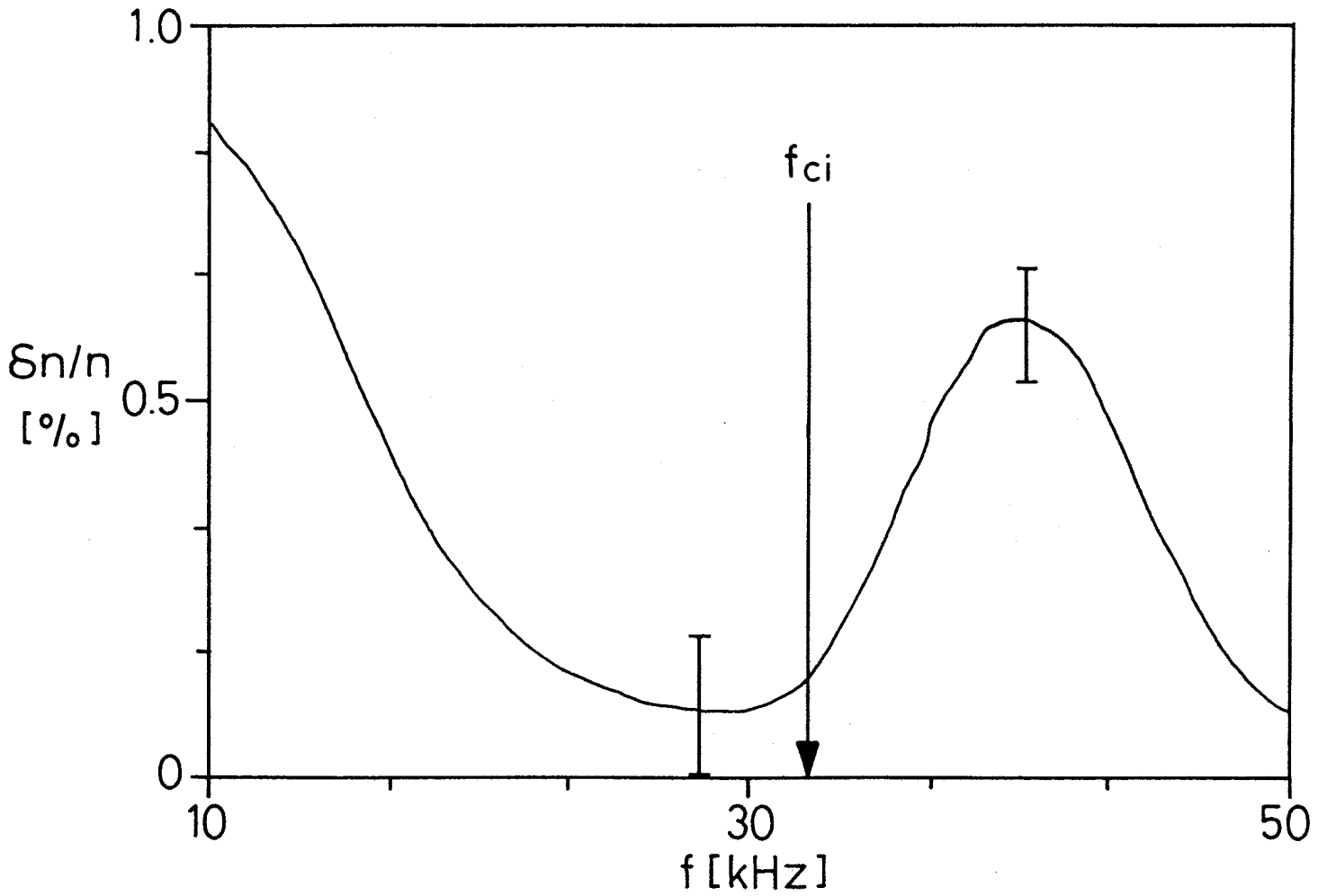

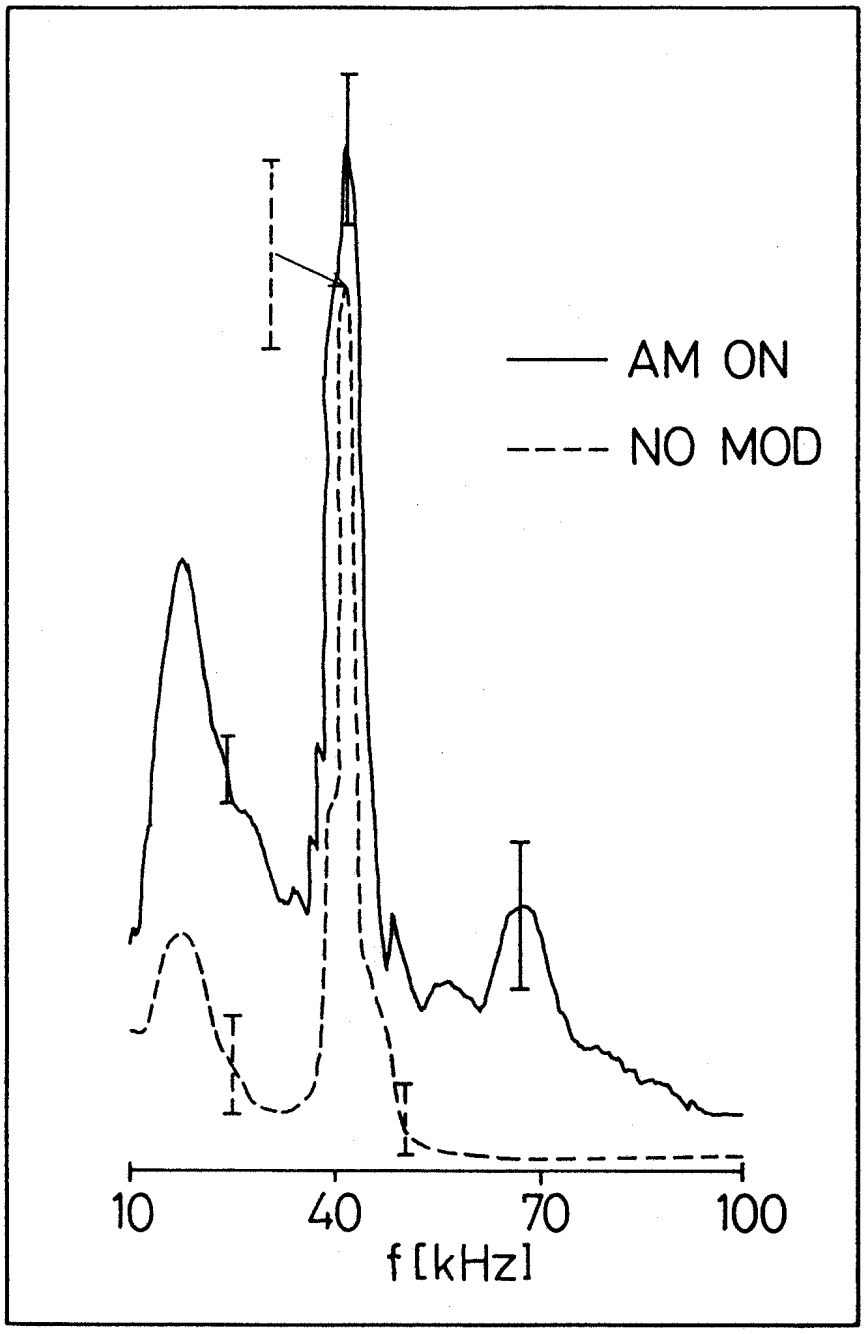

Fig. 7(b)

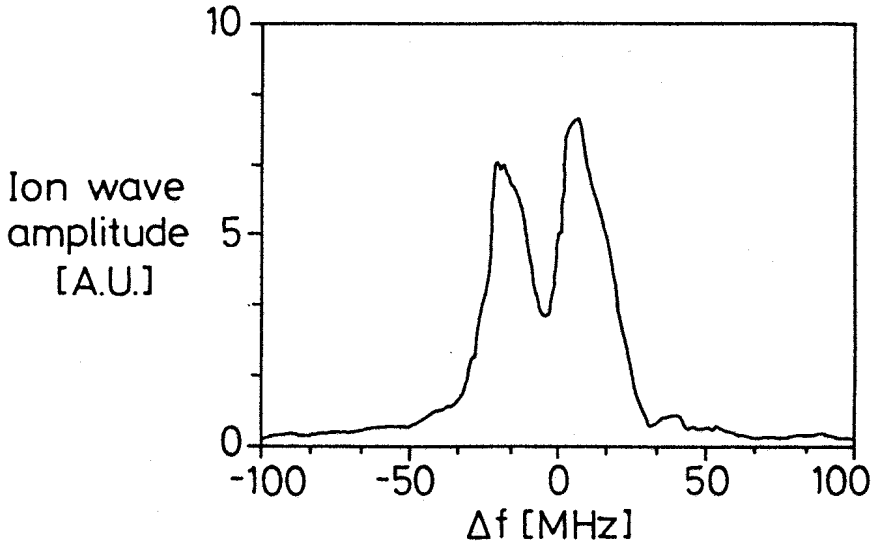

Fig. 7(c)

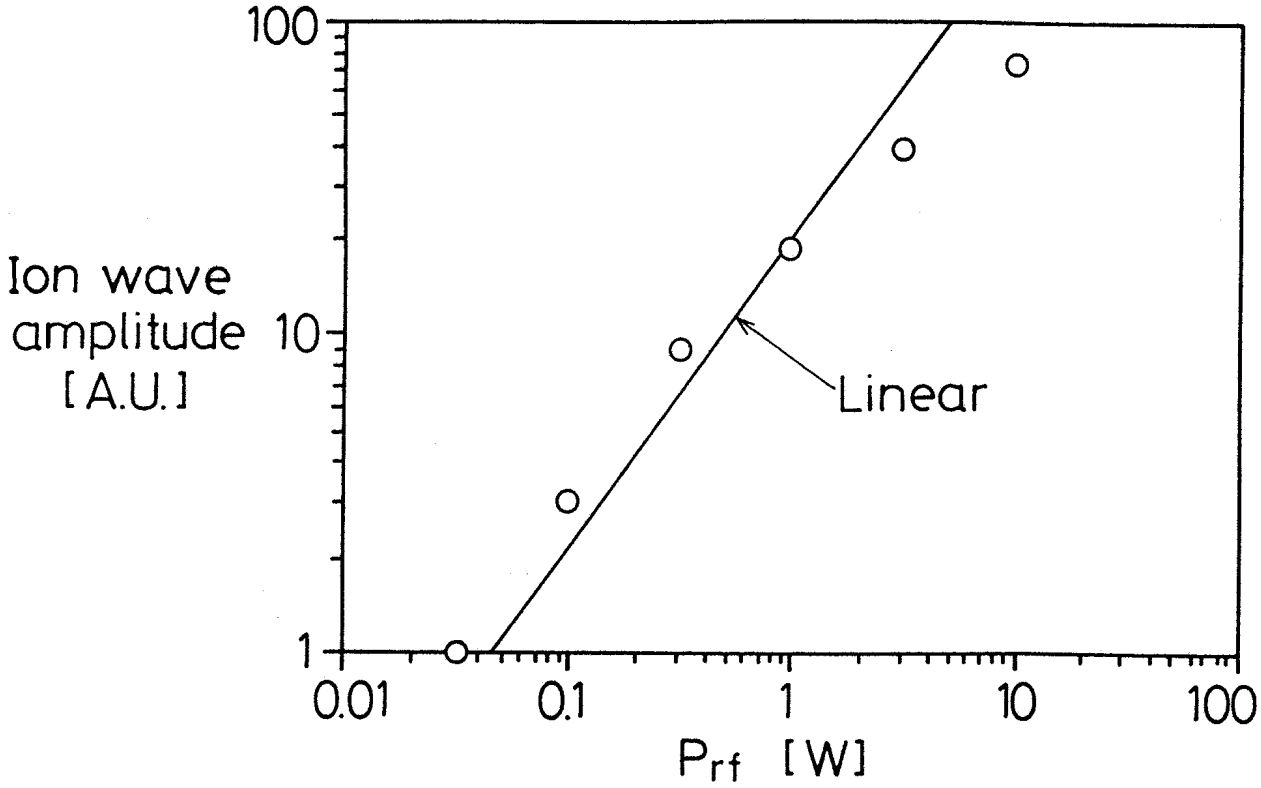

Fig. 8

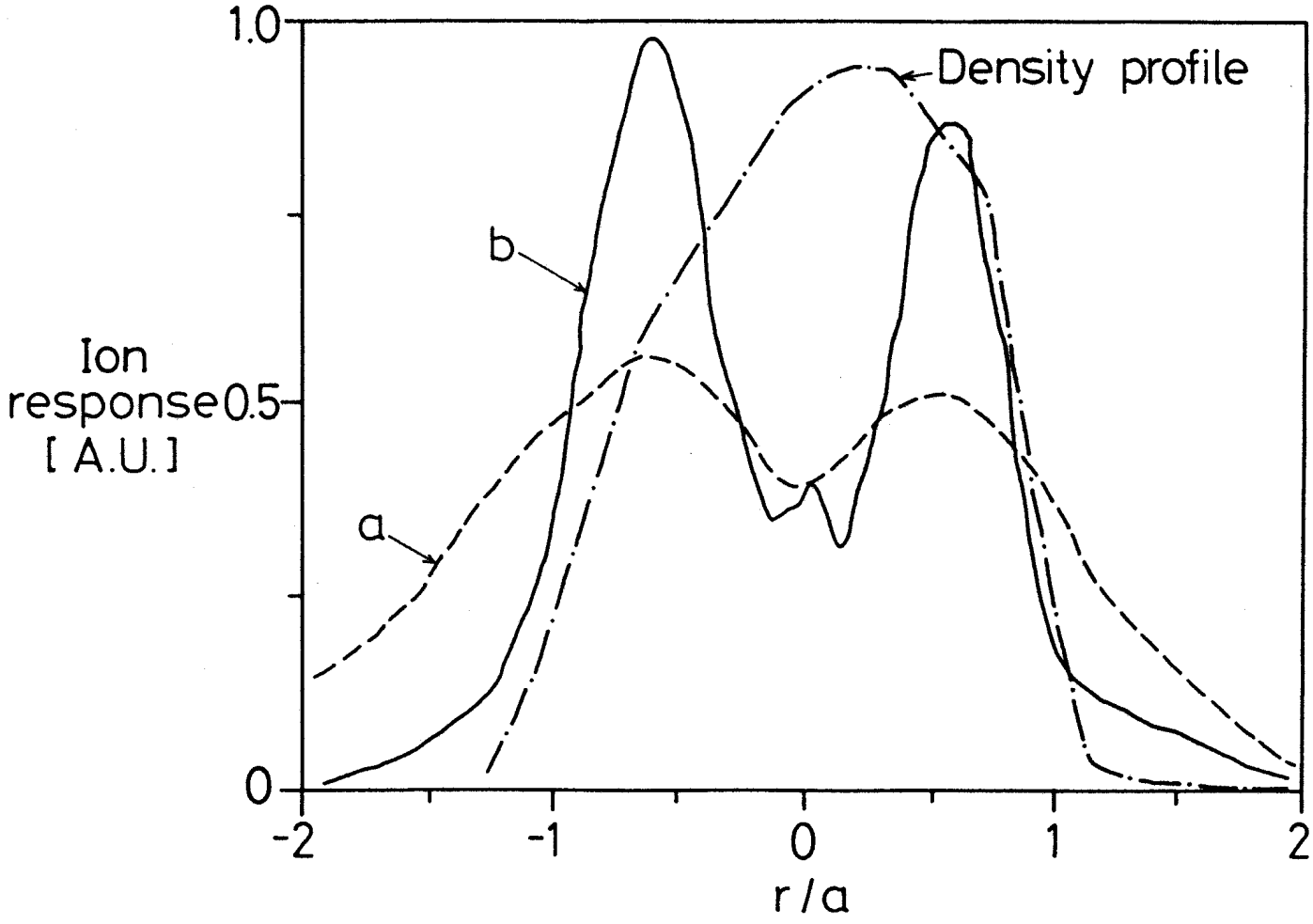

Fig. 9

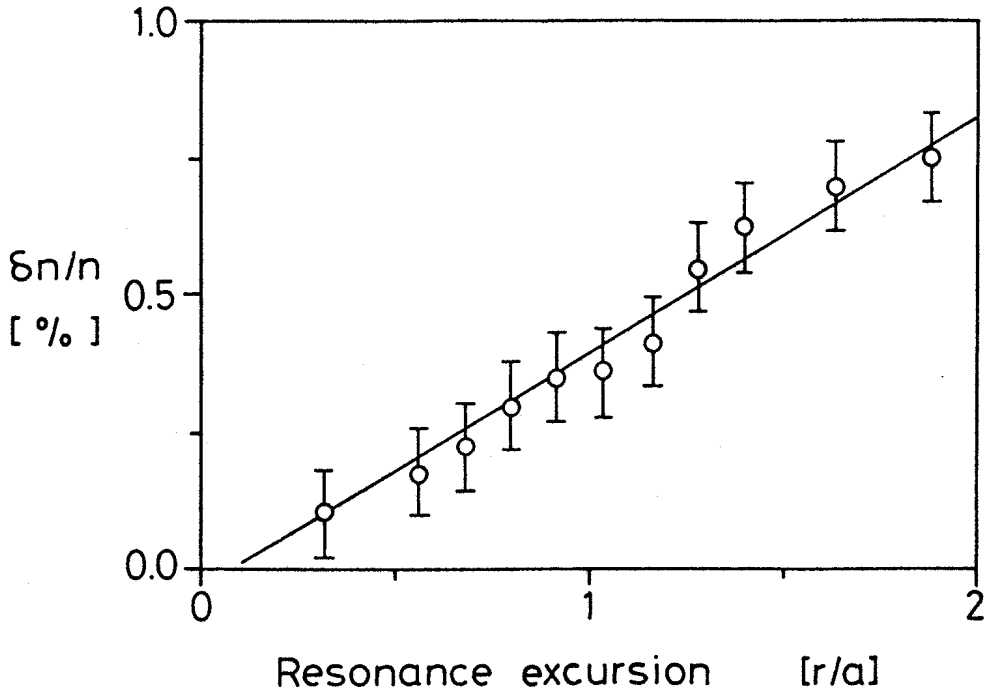

Fig. 10

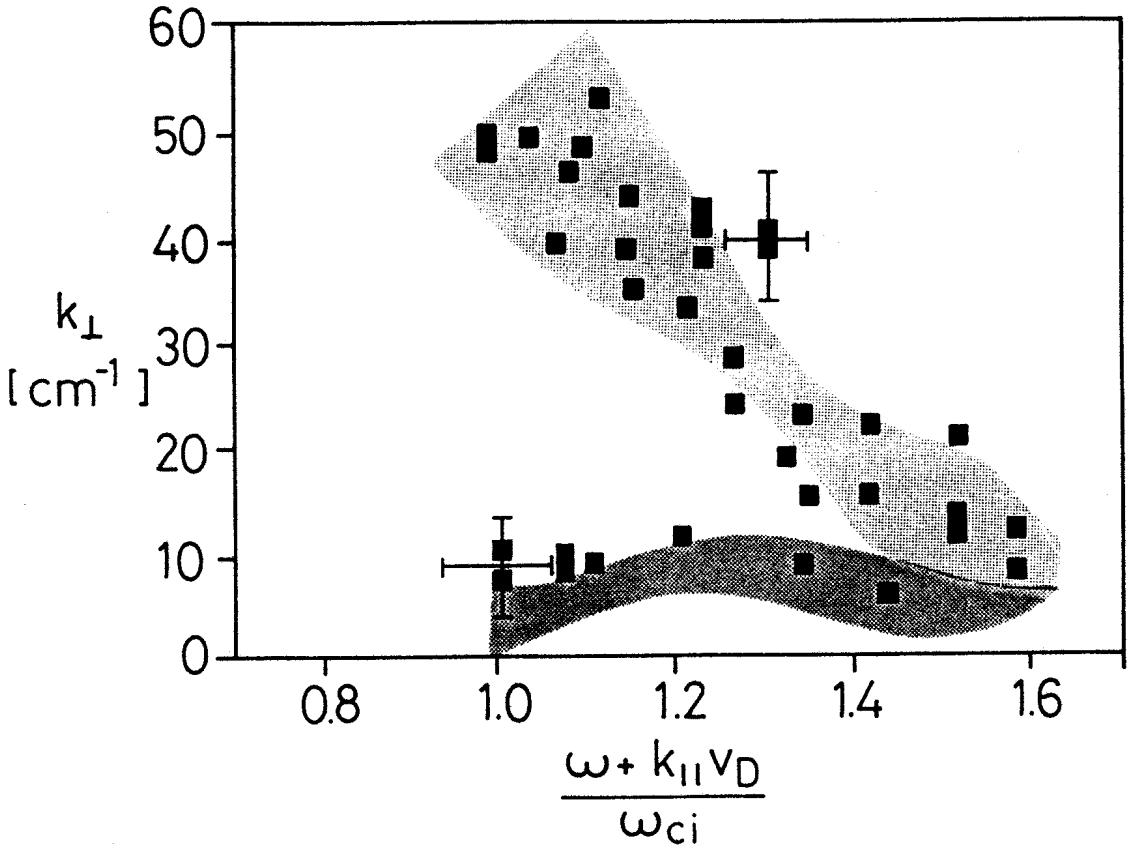
60
50
40
30
20
10
0
$k_\perp$
[cm^{-1}]
0.8
1.0
1.2
1.4
1.6
$\frac{\omega + k_{||} v_D}{\omega_{ci}}$

Fig. 11

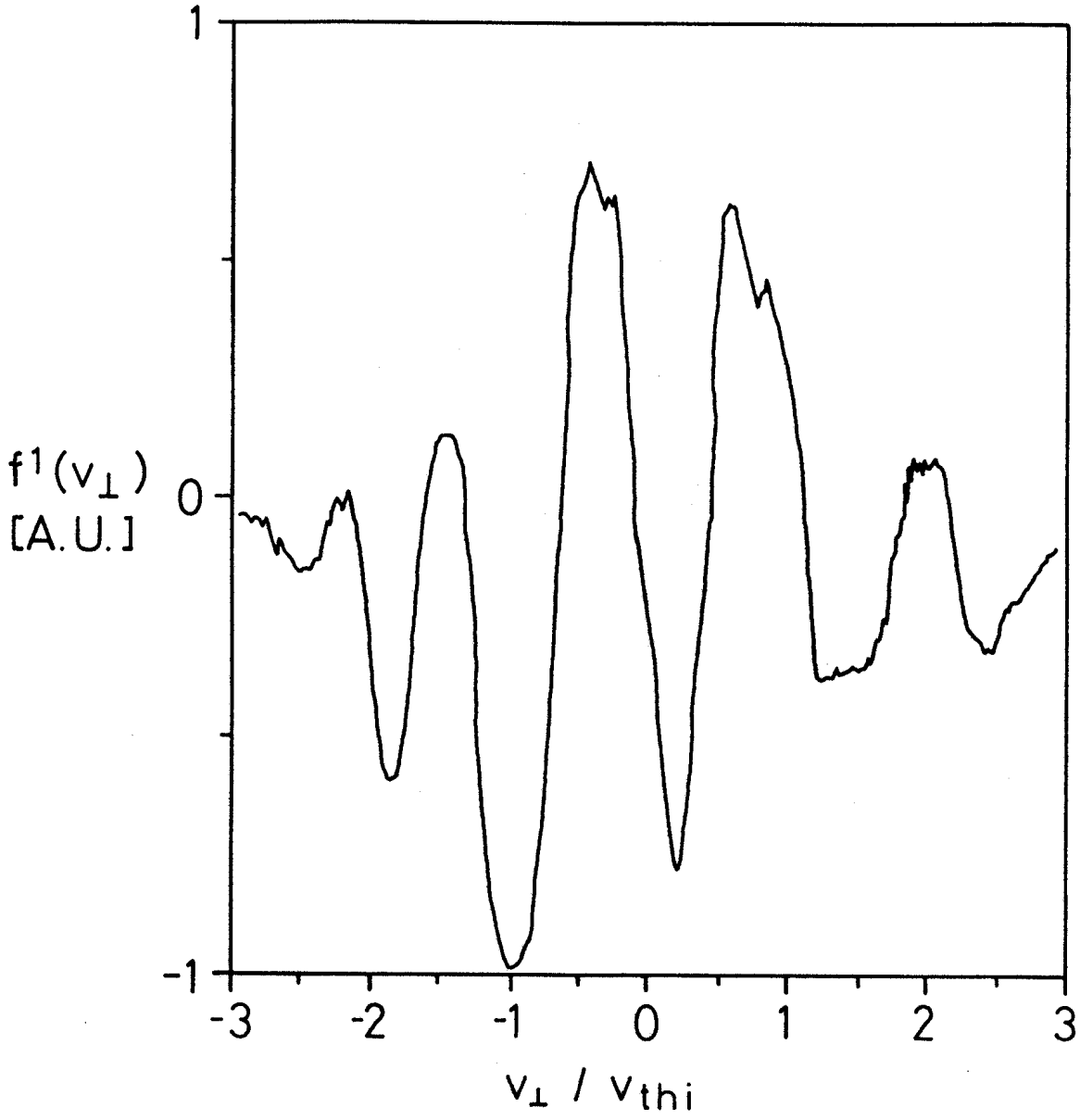

Fig. 12

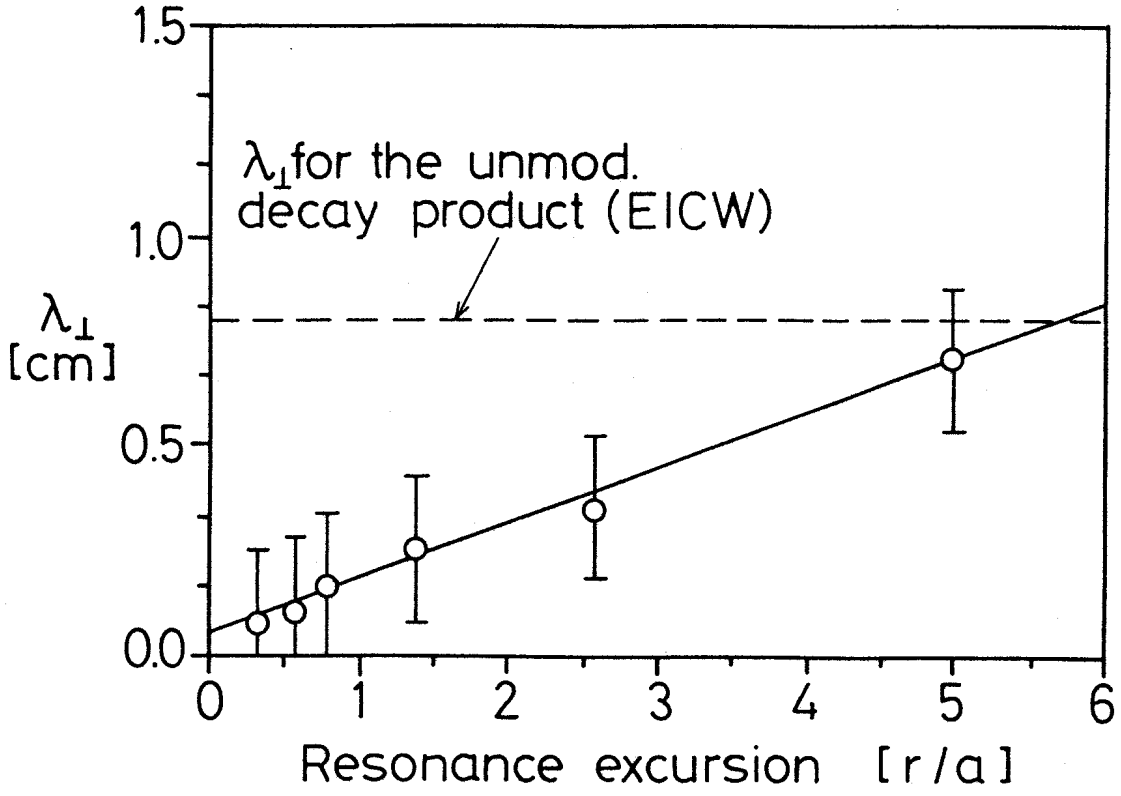
1.5
1.0
0.5
0.0
λ⊥ [cm]
λ⊥ for the unmod. decay product (EICW)
0
1
2
3
4
5
6
Resonance excursion [r/a]

Fig. 13